IJRCS

International Journal of Robotics and Control Systems
Vol. 4, No. 4, 2024, pp. 2041-2054
ISSN 2775-2658
http://pubs2.ascee.org/index.php/ijrcs

ASCEE

Design of A Backstepping Control and Synergetic Control for An Interconnected Twin-Tanks System: A Comparative Study

Rawaa Al-Majeez [a,1,*], Kareem Al-Badri [a,2], Huthaifa Al-Khazraji [a,3] , Safanah M. Ra'afat [a,4]

[a] Control and System Engineering Department, University of Technology-Iraq, Baghdad 10066, Iraq
[1] 60188@uotechnology.edu.iq; [2] 60186@uotechnology.edu.iq; [3] 60141@uotechnology.edu.iq;
[4] Safanah.m.raafat@uotechnology.edu.iq
* Corresponding Author

ARTICLE INFO

Article history
Received October 02, 2024
Revised November 05, 2024
Accepted November 16, 2024

Keywords
Nonlinear Control;
Backstepping Control;
Synergetic Control;
Twin-Tanks System;
Grasshopper Optimization Algorithm

ABSTRACT

This paper presents a comparative performance examination between designing backstepping control (BSC) and synergetic control (SC) for an interconnected twin-tanks system. The controller is used to maintain the liquid level in the tank at the desired value by manipulating the input flow rate. The nonlinear dynamics of the twin-tanks system is established first. Then, based on the nonlinear dynamics of the system, the control law of the BSC and the SC are developed. The two controllers cooperate with the grasshopper optimization algorithm (GOA) for further improvement of the control design performance by tuning the design parameters of each controller. GOA has strong searchability for optimal solution and it has been successfully used to solve several optimization problems in numerous fields. Finally, the performance and the significance of each controlled system for two case studies (normal operation and under external disturbance) are examined based on MATLAB software. The simulation data shows that the BSC gives better performance than the SC.

1. Introduction

Level control processes play a vital role in many industrial sectors, including pharmaceuticals, nuclear power plants, chemical processing, water treatment, and spray painting [1], [2]. In a twin-tank system, fluid is first pumped into the primary tank, where it is stored, and then transferred to the second tank. By manipulating the input flow rate, the controller regulates the liquid level to maintain it at a desired value.

Several researchers have investigated liquid level control in twin-tank systems. A PID (proportional_integral_derivative) controller was implemented in [3], with traditional methods used for tuning its parameters. To enhance this tuning, [4] applied a modified Ant Colony Optimization (ACO), while [5] combined PID with fuzzy logic, yielding improved performance and quality. Studies in [6] and [7] compared Sliding Mode Control (SMC) with PID, demonstrating that SMC outperforms PID in step input tracking. Similarly, [8] reported that Model Reference Adaptive Control (MRAC) achieves better transient performance than PID. To address chattering in SMC, Delavari and Noiey [9] integrated fuzzy logic and further refined the design using Genetic Algorithms (GAs), demonstrating robust disturbance rejection. Khalid and Kadri [10] explored Model Predictive Control (MPC) for stabilizing twin-tank systems under parameter variations, while [11] introduced an adaptive MRAPIDC controller to handle large disturbances. The key limitations of previous studies are:

- Most control laws rely on linearized system models, limiting accuracy.
- Physical limitations of actuators are often neglected.
- External disturbances are not adequately addressed.

To address these limitations, this paper proposes two advanced control frameworks—Backstepping Control (BSC) and Synergetic Control (SC)—for regulating the liquid level in a twin-tank system. Unlike previous studies, this work incorporates system nonlinearity, actuator saturation, and external disturbances to better reflect real-world conditions. The Grasshopper Optimization Algorithm (GOA) is employed to fine-tune the design parameters of both controllers, improving control performance.

The rest of the paper is structured as follows: Section 2 presents the mathematical modeling of the twin-tank system. Section 3 describes the development of the proposed controllers. Section 4 introduces the Grasshopper Optimization Algorithm (GOA). Section 5 reports the simulation results. Finally, Section 6 concludes the paper.

2. Mathematical Model

In the process industries, one of the fundamental issues is controlling the liquid levels between tanks. Certain industrial procedures necessitate pumping liquid, storing it in tanks, and then pumping it to another tank. Take into consideration the Fig. 1 system, which consists of twin tanks that are connected [12].

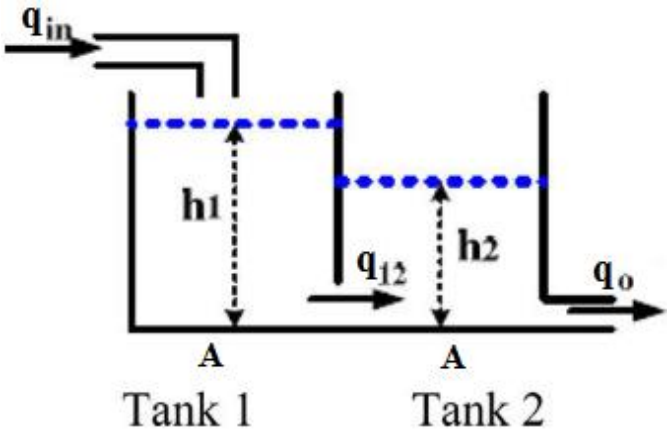

Fig. 1. Interconnected twin-tanks system

Tank 1's flow rate is q_{in} $\left(\frac{cm^3}{s}\right)$, tank 1 to tank 2's flow rate is q_{12} $\left(\frac{cm^3}{s}\right)$, and tank 2's flow rate is q_o $\left(\frac{cm^3}{s}\right)$. The liquid level heights in tanks 1 and 2 are, respectively, h_1 (cm) and h_2 (cm). The cross-sectional area of both tanks is A (cm^2). The area of the coupling orifice and the area of the outlet orifice are a_{12} and a_2 respectively. The accumulation of water in Tank 1 depends on the difference between the input flow rate to tank1 and the output flow rate from Tank 1 and the cross-sectional area of tank1 as given [4]:

$$\dot{h}_1 = \frac{q_{in} - q_{12}}{A} \tag{1}$$

The flow rate from tank1 to tank2 has a nonlinear dynamical equation as follows [5]:

$$q_{12} = a_{12}\sqrt{2g(h_1 - h_2)} \tag{2}$$

where g is the gravitational constant. The same as tank1, the accumulation water in tank 1 is given by [9]:

$$\dot{h}_2 = \frac{q_{12} - q_o}{A} \tag{3}$$

The flow rate from tank2 has the following equation [5]:

$$q_o = a_2\sqrt{2gh_2} \tag{4}$$

Substituting Eq. (2) into Eq. (1) and Eq. (4) into Eq. (3) results:

$$\dot{h}_1 = \frac{q_{in} - a_{12}\sqrt{2g(h_1 - h_2)}}{A} \tag{5}$$

$$\dot{h}_2 = \frac{a_{12}\sqrt{2g(h_1 - h_2)} - a_2\sqrt{2gh_2}}{A} \tag{6}$$

Let assume: $x_1 = h_2$, $c_1 = \frac{a_2\sqrt{2g}}{A}, c_2 = \frac{a_{12}\sqrt{2g}}{A}$, $x_2 = h_1 - h_2$ and $u = q_{in}$, Eq. (5) and Eq. (6) can be rewritten:

$$\dot{x}_1 = -c_1\sqrt{x_1} + c_2\sqrt{x_2} \tag{7}$$

$$\dot{x}_2 = \frac{u}{A} - 2c_2\sqrt{x_2} + c_1\sqrt{x_1} \tag{8}$$

In order to develop a controller, the system's mathematical model must be converted into a comparable canonical form, such the nonlinearity found in a single equation. As a result, the following new coordinates of the system are defined as follows: $z_1 = x_1$ and $z_2 = \dot{x}_1$.

Thus, the differential equations of the equivalent model in new coordinates can be expressed as:

$$\dot{z}_1 = z_2 \tag{9}$$

$$\dot{z}_2 = f(x) + g(x)\, u \tag{10}$$

where:

$$f(x) = \left(\frac{{c_1}^2 - 2{c_2}^2}{2}\right) + \frac{c_2 c_1}{2}\left(\frac{\sqrt{z_1}}{\sqrt{x_3}} - \frac{\sqrt{x_3}}{\sqrt{x_1}}\right) \tag{11}$$

$$g(x) = \frac{c_2}{2A\sqrt{x_3}} \tag{12}$$

3. Controller Design

The feedback controller has an important role in the automation system [13], [14]. There are numerous control algorithms have been designed for wide range of control systems [15]-[20]. However, backstepping control (BSC) and synergetic control (SC) techniques have gained a lot of attention due to their ability to handle different control engineering problems such as nonlinearity and ensure system stability [21], [22]. However, in the BSC approach, a virtual variable control from the first subsystem is used to stabilize the next subsystem and the same design is implemented in the next subsystem to design another virtual variable control until the dynamics of the subsystem contain the control input variable [21]. On other hand, in the SC approach, a manifold is defined as a function of the tracking error of the system. Then, the SC directs the system to move into that manifold from any initial motion point [22]. To design the

control law of both controllers, let's define the tracking error e_t as the difference between the desired level position z_d and the actual level position z_1 as follows:

$$e_t = z_d - z_1 \tag{13}$$

In the following two subsections, the procedure to develop the control law of the BSC and SC for the twin-tanks system is presented.

3.1. Backstepping Control

Based on the Lyapunov theorem, to ensure the stability of the closed-loop system, a recursive development of the backstepping control (BSC) control law is made [23]. The procedure to design the control law of the BSC is described as follows:

In the first step, let select the state z_2 as the virtual control v.

For this step, let select the L.F (Lyapunov Function) as given in Eq. (14) and taking its first time derivative as given in Eq. (15).

$$V_1 = \frac{1}{2}{e_t}^2 \tag{14}$$

$$\dot{V}_1 = e_t\dot{e}_t = e_1(\dot{z}_d - z_2) \tag{15}$$

By replacing z_2 by the virtual control v, Eq. (15) becomes:

$$\dot{V}_1 = e_1(\dot{z}_d - v) \tag{16}$$

Choose v as:

$$v = k_{bsc}e_t + \dot{z}_d \tag{17}$$

where a tuning parameter is the coefficient $k_{smc}(k_{smc} > 0)$. when Eq. (17) is substituted into (16), $\dot{V}_1$ becomes:

$$\dot{V}_1 = -k_{bsc}{e_t}^2 \tag{18}$$

Eq. (18) guarantees the exponential decrease of e_1 to zero. The error between the state z_2 and the virtual control v is defined in the second step as:

$$e_v = z_2 - v \tag{19}$$

Applying Eq. (17) of v into Eq. (19) gives:

$$e_v = z_2 - k_{bsc}e_t - \dot{z}_d \tag{20}$$

Reorganize Eq. (20) to find z_2:

$$z_2 = e_v + k_{bsc}e_t + \dot{z}_d \tag{21}$$

Take the derivative of e_v:

$$\dot{e}_v = \dot{z}_2 - k_{bsc}\dot{e}_1 - \ddot{z}_d \tag{22}$$

Choose the total L.F as:

$$V = \frac{1}{2}{e_t}^2 + \frac{1}{2}{e_v}^2 \tag{23}$$

Take the derivative of V:

$$\dot{V} = e_t\dot{e}_t + e_v\dot{e}_v \tag{24}$$

$\dot{e}_t$ from Eq. (13) and $\dot{e}_v$ from Eq. (22) can be substituted into Eq. (24) to obtain:

$$\dot{V} = e_t(\dot{z}_d - z_2) + e_v(\dot{z}_2 - k_{bsc}\dot{e}_t - \ddot{z}_d) \tag{25}$$

Rearrange Eq. (25) gives:

$$\dot{V} = -k_{bsc}{e_t}^2 + e_v\left(({k_{bsc}}^2 - 1)e_t + k_{bsc}e_v + \dot{z}_2 - \ddot{z}_d\right) \tag{26}$$

Putting the value of $\dot{z}_2$ from Eq. (10) into Eq. (26) yields:

$$\dot{V} = -k_{bsc}{e_t}^2 + e_v\left(({k_{bsc}}^2 - 1)e_t + k_{bsc}e_v + f(x) + g(x)u - \ddot{z}_d\right) \tag{27}$$

In Eq. (27) the equations $-k_{bsc}{e_1}^2$ ensure that e_t declines exponentially to zero. However, the term $\left(({k_{bsc}}^2 - 1)e_t + k_{bsc}e_v + F(x) + g(x)u - \ddot{x}_d\right)$ in Eq. (27) needs to be $-a_{bsc}{e_v}^2$, a_{bsc} ($a_{smc} > 0$) is a tuning parameter in order to ensure that e_v declines exponentially to zero.

On the basis of that, the BSC's control law can be found as follows:

$$u_{bsc} = \frac{1}{g(x)}\left(-f(x) - (a_{bsc} + k_{bsc})e_v - ({k_{bsc}}^2 - 1)e_t + \ddot{z}_d\right) \tag{28}$$

Applying the result of Eq. (28) into Eq. (27) yields:

$$\dot{V} = -k_{bsc}{e_t}^2 - a_{bsc}{e_v}^2 \tag{29}$$

The system's stability was ensured by Equation (29) and e_t and e_v will converge to zero as $t \to \infty$.

3.2. Synergetic Control

The steps to design the control law of the SC are explained as follows:

Let's define the macro-variable φ follows:

$$\varphi = k_{sc}e_t + \dot{e}_t \tag{30}$$

Taking the first-time derivative of φ obtains:

$$\dot{\varphi} = k_{sc}\dot{e}_t + \ddot{e}_t \tag{31}$$

where k_{sc} is a tunable parameter.

To guarantee the state trajectories move towards the pre-defined manifolds and remain on it for future time, the following conditions should be met:

$$\dot{\varphi} + a_{sc}\varphi = 0 \tag{32}$$

where $a_{sc} > 0$ is a tunable parameter determine the speed of convergence.

Substitute Eq. (31) in Eq. (32) gives:

$$k_{sc}\dot{e}_t + \ddot{e}_t + a_{sc}\varphi = 0 \tag{33}$$

Taking the 1st and the 2nd derivative of the e_t gives:

$$\dot{e}_t = \dot{z}_d - \dot{z}_1 = \dot{z}_d - z_2 \tag{34}$$

$$\ddot{e}_t = \ddot{z}_d - \dot{z}_2 \tag{35}$$

Substitute Eq. (10) in Eq. (35) gives:

$$k_{sc}\dot{e}_t + \ddot{z}_d - f(x) - g(x)u + a_{sc}\varphi = 0 \tag{36}$$

Solving for u

$$u_{sc} = \frac{1}{g(x)}(-f(x) + \ddot{z}_d + k_{sc}\dot{e}_t + a_{sc}\varphi) \tag{37}$$

Choose L.F as:

$$V = \frac{1}{2}\varphi^2 \tag{38}$$

Taking the first-time derivate of V obtains

$$\dot{V} = \dot{\varphi}\varphi \tag{39}$$

Substitutes $\dot{\varphi}$ as given in Eq. (25) into Eq. (30) obtains:

$$\dot{V} = -k_{sc}\varphi^2 \tag{40}$$

Eq. (40), derivative of L.F, is negative; therefore, the stability of the SC is guaranteed.

4. Grasshopper Optimization Algorithm

Swarm optimization algorithm uses an iterative and random process for solving various problems [24]-[28]. Numerous swarm optimization algorithms are available in the literature to optimize the design parameters of different controllers [29]-[36]. This paper represents grasshopper optimization algorithm (GOA) which is one of the recent swarm optimizations that used to tune the design variable of the controllers applied on the twin-tanks system. Saremi et al. [37] has introduced GOA, which has descripted the nature behavior of grasshoppers. Grasshoppers have been known for their harmful impact on crop production and agriculture. The grasshoppers are insects that travel in groups and eat the vegetation in their way. The group of grasshoppers is extremely big, which makes the framer afraid of their attack. When the grasshoppers are nymphs, they are wingless move slowly in the direction of wind like rolling cylinders. When they are adults, they gather in swarms to fly in the air and cover a long distance [38]. The nature of grasshoppers inspired the researchers to divide the process into exploration and exploitation along with target seeking. There is a difference in movement between these two functions. The agents move unexpectedly in exploration, while they move locally in exploitation. The travel nature of the grasshoppers can be mathematically modeled as follow [37]:

$$X_i = S_i + G_i + A_i \tag{41}$$

where X_i define the position of i-th grasshopper, S_i is the social interaction, G_i is the gravity force, and A_i is the wind advection. This equation can provide a random behavior of grasshoppers by multiplying the equation with the random number r in the range of $[0,1]$ as follow:

$$X_i = rS_i + rG_i + rA_i \tag{42}$$

Social interaction S_i can be affected by other parameters, as it is shown in the equations [36]:

$$S_i = \sum_{\substack{j=1 \\ j\neq i}}^{N} s(d_{ij})\widehat{d_{ij}} \tag{43}$$

$$s(r) = fe^{-r/l} - e^{-r} \tag{44}$$

$$d_{ij} = |x_j - x_i| \tag{45}$$

$$\widehat{d_{ij}} = \frac{x_j - x_i}{d_{ij}} \tag{46}$$

It can be seen that the social interaction equation consists of s which is the strength of social forces and is defined in Eq. (44). In Eq. (44), f is the intensity of attraction, and l is the attractive length scale and d_{ij} represents the distance between two grasshoppers' i-th and j-th as shown in Eq. (45). Eq. (46) defines the unit vector $\widehat{d_{ij}}$ from i-th to j-th grasshoppers.

It has been shown that *s* function affects the social interaction where any change in f and l leads to impacts on the strength of social force and then the social interaction, attraction, repulsion, and comfort zone of the grasshoppers. The social interaction was the reason for modeling the grasshopper's group through the impact of its function on comfort zone and grasshoppers' positions. The space between any two grasshoppers divided into repulsion, attraction, and comfort zones. The distance mapped into small intervals in case that the distance between two grasshoppers is long.

For gravity force G_i , it can be calculated as shown in Eq. (47):

$$G_i = -g\widehat{e_g} \tag{47}$$

where g is the gravitational constant, and $\widehat{e_g}$ is the unity vector toward the earth's center. The last term in the position Eq. (41) is the wind advection that can be written as follow:

$$A_i = \rho\widehat{e_w} \tag{48}$$

where ρ is a constant, and $\widehat{e_w}$ is a unity vector in wind direction.

By substituting S_i, G_i , and A_i in Eq. (41) gives:

$$X_i = \sum_{\substack{j=1 \\ j\neq i}}^{N} s(|x_j - x_i|)\frac{x_j - x_i}{d_{ij}} - g\widehat{e_g} + \rho\widehat{e_w} \tag{49}$$

By implementing equation (49), the grasshoppers have shown to reach their comfort zone and do not leave it. This led to a frailer in the exploration and exploitation process toward the solution. Therefore, this mathematical model cannot be applied to the optimization problem, so a modified version of this equation has been proposed as shown in Eq. (50) [37]:

$$X_i^d = c\left(\sum_{\substack{j=1 \\ j\neq i}}^{N} c\frac{ub_d - lb_d}{2} s(|x_j^d - x_i^d|)\frac{x_j - x_i}{d_{ij}}\right) + \widehat{T_d} \tag{50}$$

where S_i is almost the same, G_i did not consider, and A_i is assumed to be toward the target $\widehat{T_d}$. ub_d is the upper bond and lb_d is the lower bond in D-th dimension. $\widehat{T_d}$ is the value of the D-th dimension, and c is the decreasing coefficient to reduce the comfort zone, repulsion region, and attraction region. $\widehat{T_d}$ demonstrates the grasshopper's movement tendency to the target. The rest of Eq. (50) characterizes the interaction between grasshoppers considering the position of others.

In Eq. (50), the first term represents the location of the current grasshopper with respect to other grasshoppers. This algorithm is different from other optimization algorithms. To update the position of grasshoppers in GOA, the current position, target position, and all other grasshoppers' positions are utilized. Also, GOA has only one vector for each search agent, while another optimization has two vectors for velocity and position.

It could be noticed that there are two c in Eq. (50), each one has its own purpose. The first c on the left works as the inertial weight in PSO. It is responsible for balancing the movement of grasshoppers in exploration and exploitation processes around the target while the iteration increases. On the other hand, the inner c works to reduce the repulsion, attraction region, and comfort zone between grasshoppers, and the iteration number decreases. GOA starts with the exploration process to find the appropriate searching spaces, and then the exploitation process sends the agent to search locally to find the global optimum opposite to the real nature of the grasshopper's movement. Therefore, parameter c is utilized to balance the process of exploration and exploitation as shown in Eq. (51) [39]:

$$\mathrm{c} = c_{max} - \mathrm{l}\frac{c_{max} - c_{min}}{\mathrm{L}} \tag{51}$$

where $c_{max}$is the maximum value of c which is set to 1, $c_{min}$is the minimum value of c which is set to 0.00001, l is the current iteration, and L is the maximum number of iterations. To find the global optimal solution in GOA, the grasshoppers move toward the grasshopper with the best value in each iteration. This would lead to the best approximate optimal real solution in searching space.

5. Numerical Results

The twin-tank system's close loop with each controller coded in MATLAB is used to assess the effectiveness of the BSC and the SC. Table 1 [9] contains an overview of the system's parameters. Tank 2 had a starting level of 0.01 cm and a goal level of 5 cm. The input flow rate is saturated between 0 and 150 cm^3/s because of the physical actuator restriction.

Table 1. Parameters of twin-tanks system

Parameters	Values
Cross-section area (A)	200 cm^2
Area of the coupling orifice (a_{12})	0.2 cm^2
Area of the outlet orifice (a_2)	0.25 cm^2
Gravitational constant (g)	981 cm/s^2

The tuning parameters of each controller, ($\mathrm{k_{bsc}}$and $\mathrm{a_{bsc}}$) in Eq. (20) for the BSC and ($\mathrm{k_{sc}}$ and $\mathrm{a_{sc}}$) in Eq. (39) for the SC, are adjusted using the GOA in order to ensure optimal performance. The GOA optimized the performance of the two controllers based on an error index that is named the Root Mean Square Error (RMSE) as defined in Eq. (52) [40]. The RMSE metric are wide used to assess the control performance [41].

$$\mathrm{RMSE} = \sqrt{\frac{1}{\mathrm{n}}\sum_{\mathrm{m}=1}^{\mathrm{n}} \mathrm{e_t}^2} \tag{52}$$

where n is the number of samples in the simulation and e_t is the tracking error. Table 2 reports the parameters of the GOA. Fig. 2 illustrates the convergence of the GOA algorithm used to find the optimal controller setting. Table 3 contains a list of the controllers' design parameters and their values. Fig. 3 and Fig. 4 show the control law and the system's response of the two controlled systems, respectively. Table 4 reports the corresponding numerical value of the RMSE.

Table 2. Parameters of GOA

Parameters	Values
The size of the population (N)	25
The number of iterations (L)	40

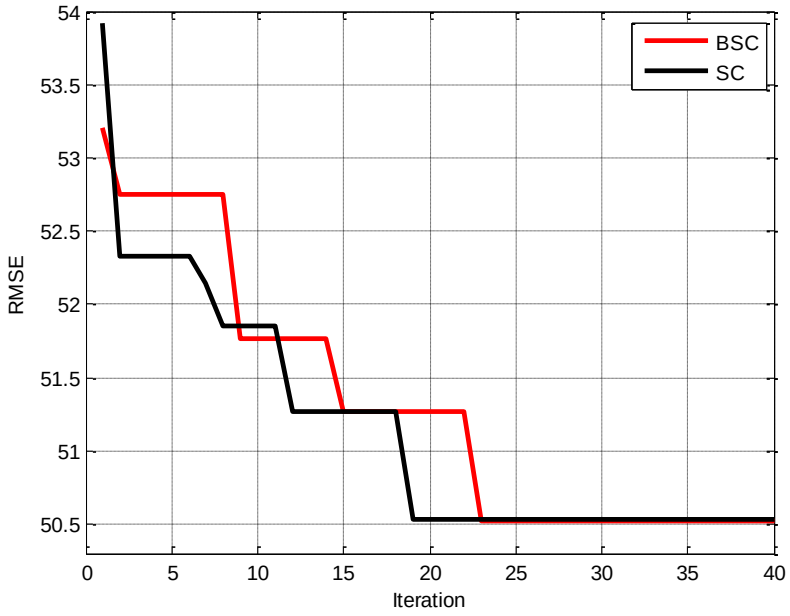

Fig. 2. Convergence of GTO for the two controllers

Table 3. The optimal value of the controllers' tuning parameters based on GOA

Controller	Parameters	Values
BSC	k_{bsc}	0.7
	a_{bsc}	2.8
SC	k_{sc}	0.42
	a_{sc}	0.8

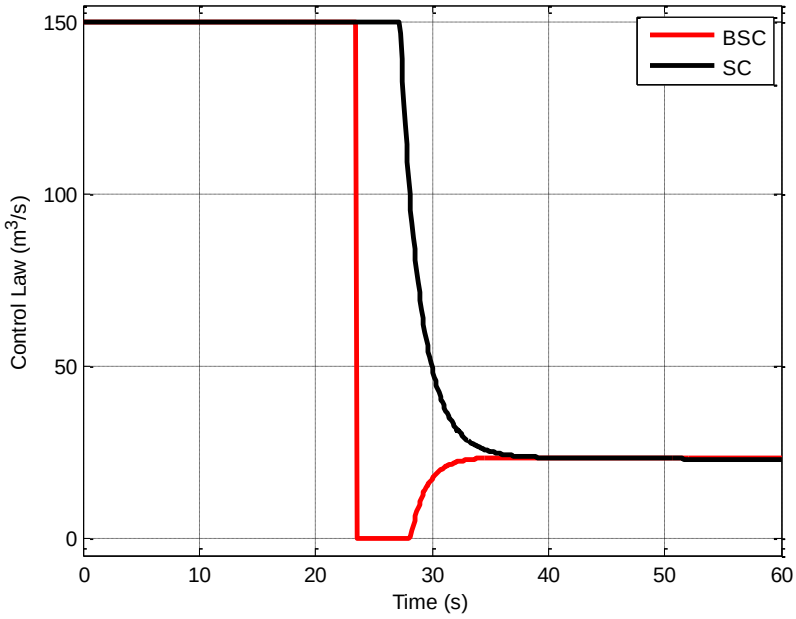

Fig. 3. Control signals for both BSC and SC with actuator saturation applied

From Fig. 3, it can be observed that the control signals for the two controllers have been saturated based on the allowable range of the actuator. Moreover, in Fig. 4, it can be seen that the

BSC controller has achieved a faster response than that of the SC. This result is confirmed by the numerical data in Table 4. The value of settling time (t_s) reduces from 31s for the SC to 27s for the BSC. Moreover, the value of the RMSE index for the BSC controller (50.52cm) is less than the value of the RMSE index for the SC controller (50.53cm).

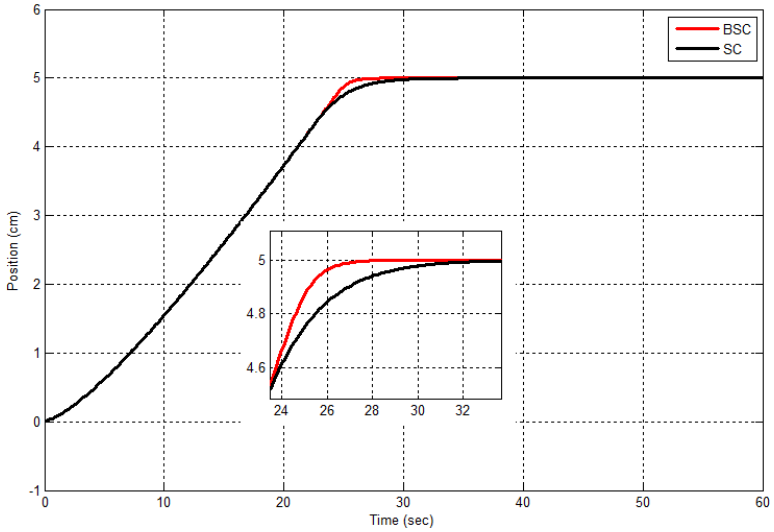

Fig. 4. System's response

Table 4. RMSE index

Index	BSC	SC
RMSE (cm)	50.52	50.53
t_s (s)	27	31

It is assumed that the system experiences a step disturbance at 40 s into the simulation duration in order to assess the suggested controller's ability to reject disturbances. The two regulated systems' behavior in track the intended output while experiencing disturbances is depicted in Fig. 5. The recovery time (t_{rec}) and the difference between the steady state and minimum amplitude of the response under disturbance (δ) are used to assess how well the controlled system performs in the disturbance scenario. Table 5 reports the dynamic response of the two controllers with disturbance.

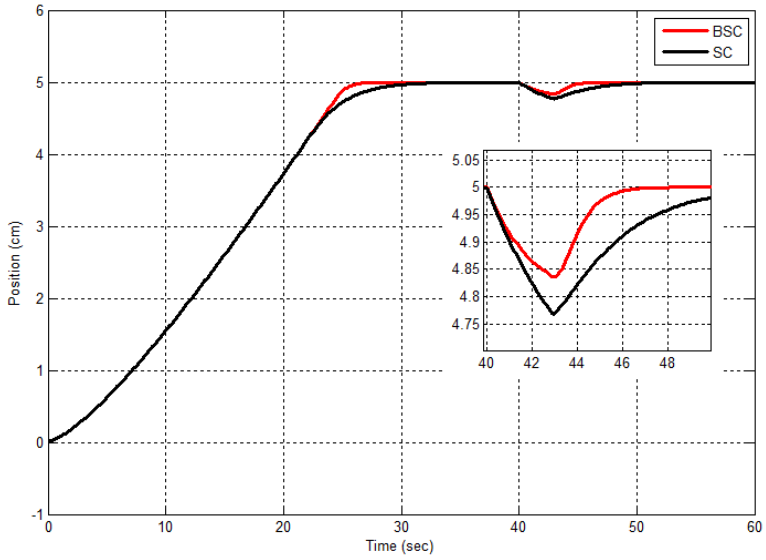

Fig. 5. System's response under disturbance

By comparing the performance of the BSC and SC, using Fig. 5 and Table 5, it can be seen that BSC's disturbance rejection minimizes deviation more effectively, with less oscillation than that of the SC. The value of t_{rec} is reduced from 10s for the SC to 6s for the BSC. Besides, the δ value is reduced from 0.25cm for the SC to 0.15cm for the BSC. This leads to the conclusion that the BSC is more robust against external disturbance than the SC.

Table 5. RMSE index under disturbance

Index	BSC	SC
RMSE (cm)	0.15	0.25
t_{rec} (s)	6	10

6. Conclusion

An interconnected twin-tank system was the subject of a comparison study in this research between backstepping control (BSC) and synergetic control (SC). The way to develop the two controllers was provided, and the system's mathematical model was established. To change the suggested controllers' modifiable parameters, the grasshopper optimization technique has been carried out. The system with the two optimized controllers was programmed in MATLAB. The controllers were stable which proved with Lyapunov stability theory and the simulation. However, it was observed that the BSC has better control characteristics than the SC control. In terms of the response's speed, the BSC improved the settling time by 12.9% as compared to the SC. In the context of robustness against disturbance, the BSC improved the recovery time by 40% as compared to the SC.

For future work, this study can be extended by including alternative optimization algorithms for the purpose of comparison with the proposed grasshopper optimization algorithm technique. Moreover, using other nonlinear controllers could be also other extension of this paper. Finally, applying the proposed control algorithm for more complex multi-tank systems can be consider another direction for future work.

Author Contribution: All authors contributed equally to the main contributor to this paper. All authors read and approved the final paper.

Funding: This research received no external funding.

Conflicts of Interest: The authors declare no conflict of interest.

Nomenclature

q_{in}	The flow input	X_i	the position of i-th grasshopper
q_{12}	The flow to the second tank	S_i	the social interaction
A	The area of tank 1,2	G_i	the gravity force
a_{12}	The coupling orifice	A_i	the wind advection
g	The gravitational constant	s	the strength of social forces
h_1	The height in tank one	d_{ij}	the distance between two grasshoppers
h_2	The height in tank two	$\widehat{d_{ij}}$	the unit vector
q_o	The flow output	f	the intensity of attraction
a_2	The outlet orifice	l	the attractive length scale
e_t	The tracking error	r	random number
z_d	The desired level position	$\widehat{e_g}$	the unity vector toward the earth center
z_1	The actual level position	$\widehat{e_w}$	unity vector in wind direction.
V_1	first Lyapunov function	ub_d	the upper bond
v	The virtual control	lb_d	the lower bond
k_{bsc}	The constant of backstepping control	c	the decreasing coefficient
e_v	The error of virtual control	$\widehat{T_d}$	the value of D-th dimension
V	Total Lyapunov function	c_{max}	maximum value of c
u_{bsc}	The control law of the BSC	c_{min}	minimum value of c

a_{bsc}	The tuning parameter of the BSC	L	the maximum number of iterations
a_{sc}	an adjustable parameter	RMSE	the Root Mean Square Error
k_{sc}	scalar design parameter of SC		

Greek symbols

Φ	macro-variable
P	a constant in wind advection

Subscripts

In	Input
O	Output
T	Tracking
D	Desired
Bsc	Backstepping control
Sc	Synergetic control
V	Virtual
i, j	Counter of the grasshoppers
g	Earth center (gravitational)
w	wind
b_d	bond in D-th dimension

References

[1] H. Gouta, S. H. Said, N. Barhoumi, and F. M'Sahli, "Observer-based backstepping controller for a state-coupled two-tank system," *IETE Journal of Research*, vol. 61, no. 3, pp. 259-268, 2015, https://doi.org/10.1080/03772063.2015.1018846.

[2] H. Pan, H. Wong, V. Kapila, and M. S. de Queiroz, "Experimental validation of a nonlinear backstepping liquid level controller for a state coupled two tank system," *Control Engineering Practice*, vol. 13, no. 1, pp. 27-40, 2005, https://doi.org/10.1016/j.conengprac.2003.12.019.

[3] M. A. Fellani and A. M. Gabaj, "PID controller design for two tanks liquid level control system using Matlab," *International Journal of Electrical and Computer Engineering (IJECE)*, vol. 5, no. 3, p. 436, 2015, http://doi.org/10.11591/ijece.v5i3.pp436-442.

[4] S. Chauhan, B. Singh, and M. Singh, "Modified ant colony optimization based PID controller design for coupled tank system," *Engineering Research Express*, vol. 3, no. 4, p. 045005, 2021, https://doi.org/10.1088/2631-8695/ac2bf3.

[5] T. L. Mien, "Liquid level control of coupled-tank system using fuzzy-PID controller," *International Journal of Engineering Research & Technology*, vol. 16, no. 11, pp. 459-464, 2017, https://www.ijert.org/liquid-level-control-of-coupled-tank-system-using-fuzzy-pid-controller.

[6] T. Toms and D. Hepsiba, "Comparison of PID controller with a sliding mode controller for a coupled tank system," *International Journal of Engineering Research & Technology*, vol. 3, no. 2, pp. 151-154, 2014, https://www.ijert.org/research/comparison-of-pid-controller-with-a-sliding-mode-controller-for-a-coupled-tank-system-IJERTV3IS20135.pdf.

[7] B. J. Parvat, V. K. Jadhav, and N. N. Lokhande, "Design and implementation of sliding mode controller for level control," *IOSR Journal of Electronics and Communication Engineering*, vol. 2, pp. 51-54, 2012, https://iosrjournals.org/iosr-jece/papers/sicete-volume1/12.pdf.

[8] G. Nandhinipriyanka, S. Ishwarya, S. Janakiraman, C. S. Thana, and P. Vaishali, "Design of model reference adaptive controller for cylinder tank system," *International Journal of Pure and Applied Mathematics*, vol. 118, no. 20, pp. 2007-2013, 2018, https://acadpubl.eu/jsi/2018-118-20/articles/20c/93.pdf.

[9] H. Delavari and A. R. Noiey, "Genetic-based Fuzzy Sliding Mode Control of an Interconnected Twin-Tanks," *EUROCON 2007 - The International Conference on "Computer as a Tool"*, pp. 714-719, 2007, https://doi.org/10.1109/EURCON.2007.4400597.

[10] M. U. Khalid and M. B. Kadri, "Liquid level control of nonlinear Coupled Tanks System using linear model predictive control," *2012 International Conference on Emerging Technologies*, pp. 1-5, 2012, https://doi.org/10.1109/ICET.2012.6375434.

[11] Y. D. Mfoumboulou, "Design of a model reference adaptive PID control algorithm for a tank system," *International Journal of Electrical and Computer Engineering (IJECE)*, vol. 11, no. 1, pp. 300-318, 2021, http://doi.org/10.11591/ijece.v11i1.pp300-318.

[12] H. Delavari, R. Ghaderi, A. Ranjbar, and S. Momani, "Fuzzy fractional order sliding mode controller for nonlinear systems," *Communications in Nonlinear Science and Numerical Simulation*, vol. 15, no. 4, pp. 963-978, 2010, https://doi.org/10.1016/j.cnsns.2009.05.025.

[13] Z. N. Mahmood, H. Al-Khazraji, and S. M. Mahdi, "PID-based enhanced flower pollination algorithm controller for drilling process in a composite material," *Annales de Chimie. Science des Materiaux*, vol. 47, no. 2, pp. 91-96, 2023, https://doi.org/10.18280/acsm.470205.

[14] H. Al-Khazraji, C. Cole, and W. Guo, "Dynamics analysis of a production-inventory control system with two pipelines feedback," *Kybernetes*, vol. 46, no. 10, pp. 1632-1653, 2017, https://doi.org/10.1108/K-04-2017-0122.

[15] R. M. Naji, H. Dulaimi, and H. Al-Khazraji, "An optimized PID controller using enhanced bat algorithm in drilling processes," *Journal Européen des Systèmes Automatisés*, vol. 57, no. 3, pp. 767-772, 2024, https://doi.org/10.18280/jesa.570314.

[16] M. A. Al-Ali, O. F. Lutfy, and H. Al-Khazraj, "Investigation of optimal controllers on dynamics performance of nonlinear active suspension systems with actuator saturation," *Journal of Robotics and Control*, vol. 5, no. 4, pp. 1041-1049, 2024, https://doi.org/10.18196/jrc.v5i4.22139.

[17] V. I. Lachin, V. S. Elsukov and M. N. Mustafa, "Synthesis of robust automatic control system of electromagnetic bearings," *2015 International Siberian Conference on Control and Communications (SIBCON)*, pp. 1-4, 2015, https://doi.org/10.1109/SIBCON.2015.7147050.

[18] A. K. Ahmed and H. Al-Khazraji, "Optimal control design for propeller pendulum systems using gorilla troops optimization," *Journal Européen des Systèmes Automatisés*, vol. 56, no. 4, pp. 575-582, 2023, https://doi.org/10.18280/jesa.560407.

[19] H. Al-Khazraji, C. Cole, and W. Guo, "Analysing the impact of different classical controller strategies on the dynamics performance of production-inventory systems using state space approach," *Journal of Modelling in Management*, vol. 13, no. 1, pp. 211-235, 2018, https://doi.org/10.1108/JM2-08-2016-0071.

[20] M. N. Mustafa, "Simulation of electromagnetic suspension functioning processes in the MATLAB/Simulink system," *Journal of Physics: Conference Series*, vol. 2060, no. 1, p. 012028, 2021, https://doi.org/10.1088/1742-6596/2060/1/012028.

[21] H. Al-Khazraji, R. M. Naji, and M. K. Khashan, "Optimization of sliding mode and back-stepping controllers for AMB systems using gorilla troops algorithm," *Journal Européen des Systèmes Automatisés*, vol. 57, no. 2, pp. 417-424, 2024, https://doi.org/10.18280/jesa.570211.

[22] E. Santi, A. Monti, Donghong Li, K. Proddutur and R. A. Dougal, "Synergetic control for DC-DC boost converter: implementation options," *IEEE Transactions on Industry Applications*, vol. 39, no. 6, pp. 1803-1813, 2003, https://doi.org/10.1109/TIA.2003.818967.

[23] M. F. Badr, E. H. Karam, and N. M. Mjeed, "Control design of damper mass spring system based on backstepping controller scheme," *International Review of Applied Sciences and Engineering*, vol. 11, no. 2, pp. 181-187, 2020, https://doi.org/10.1556/1848.2020.20049.

[24] H. Al-Khazraji, W. Guo, A. J. Humaidi, "Improved cuckoo search optimization for production inventory control systems," *Serbian Journal of Electrical Engineering*, vol. 21, no. 2, pp. 187-200, 2024, https://doi.org/10.2298/SJEE2402187A.

[25] H. Al-Khazraji, "Comparative study of whale optimization algorithm and flower pollination algorithm to solve workers assignment problem," *International Journal of Production Management and Engineering*, vol. 10, no. 1, pp. 91-98, 2022, https://doi.org/10.4995/ijpme.2022.16736.

[26] H. Al-Khazraji, S. Khlil, and Z. Alabacy, "Cuckoo search optimization for solving product mix problem," *IOP Conference Series: Materials Science and Engineering*, vol. 1105, no. 1, pp. 1-9, 2021, https://doi.org/10.1088/1757-899X/1105/1/012016.

[27] S. Khlil, H. Al-Khazraji, and Z. Alabacy, "Solving assembly production line balancing problem using greedy heuristic method," *IOP Conference Series: Materials Science and Engineering*, vol. 745, no. 1, pp. 1-7, 2020, https://doi.org/10.1088/1757-899X/745/1/012068.

[28] F. Alhamudi, J. N. Elquthb, Qurtubi and I. P. Rachmadewi, "Analysis of Competitiveness and Halal Logistics of Small and Medium Industry in Beverage," *2023 International Conference On Cyber Management And Engineering (CyMaEn)*, pp. 103-107, 2023, https://doi.org/10.1109/CyMaEn57228.2023.10051071.

[29] Z. N. Mahmood, H. Al-Khazraji, and S. M. Mahdi, "Adaptive control and enhanced algorithm for efficient drilling in composite materials," *Journal Européen des Systèmes Automatisés*, vol. 56, no. 3, pp. 507-512, 2023, https://doi.org/10.18280/jesa.560319.

[30] R. A. Kadhim, M. Q. Kadhim, H. Al-Khazraji, and A. J. Humaidi, "Bee algorithm based control design for two-links robot arm systems," *IIUM Engineering Journal*, vol. 25, no. 2, pp. 367-380, 2024, https://doi.org/10.31436/iiumej.v25i2.3188.

[31] A. K. Ahmed, H. Al-Khazraji, and S. M. Raafat, "Optimized PI-PD control for varying time delay systems based on modified Smith predictor," *International Journal of Intelligent Engineering and Systems*, vol. 17, no. 1, pp. 331-342, 2024, https://doi.org/10.22266/ijies2024.0229.30.

[32] H. Al-Khazraji, K. Al-Badri, R. Al-Majeez, and A. J. Humaidi, "Synergetic control design based sparrow search optimization for tracking control of driven-pendulum system," *Journal of Robotics and Control*, vol. 5, no. 5, pp. 1549-1556, 2024, https://doi.org/10.18196/jrc.v5i5.22893.

[33] F. R. Yaseen, M. Q. Kadhim, H. Al-Khazraji, and A. J. Humaidi, "Decentralized control design for heating system in multi-zone buildings based on whale optimization algorithm," *Journal Européen des Systèmes Automatisés*, vol. 57, no. 4, pp. 981-989, 2024, https://doi.org/10.18280/jesa.570406.

[34] H. Al-Khazraji, K. Al-Badri, R. Almajeez, and A. J. Humaidi, "Synergetic control-based sea lion optimization approach for position tracking control of ball and beam system," *International Journal of Robotics and Control Systems*, vol. 4, no. 4, pp. 1547-1560, 2024, https://doi.org/10.31763/ijrcs.v4i4.1551.

[35] M. Q. Kadhim, F. R. Yaseen, H. Al-Khazraji and A. J. Humaidi, "Application of Terminal Synergetic Control Based Water Strider Optimizer for Magnetic Bearing Systems," *Journal of Robotics and Control*, vol. 5, no. 6, pp. 1973-1979, 2024, https://doi.org/10.31763/ijrcs.v4i4.1551.

[36] F. R. Al-Ani, O. F. Lutfy and H. Al-Khazraji, "Optimal Backstepping and Feedback Linearization Controllers Design for Tracking Control of Magnetic Levitation System: A Comparative Study," *Journal of Robotics and Control*, vol. 5, no. 6, pp. 1888-1896, 2024, https://doi.org/10.18196/jrc.v5i6.24073.

[37] S. Saremi, S. Mirjalili, and A. Lewis, "Grasshopper optimisation algorithm: theory and application," *Advances in Engineering Software*, vol. 105, pp. 30-47, 2017, https://doi.org/10.1016/j.advengsoft.2017.01.004.

[38] Y. Meraihi, A. B. Gabis, S. Mirjalili and A. Ramdane-Cherif, "Grasshopper Optimization Algorithm: Theory, Variants, and Applications," *IEEE Access*, vol. 9, pp. 50001-50024, 2021, https://doi.org/10.1109/ACCESS.2021.3067597.

[39] S. Z. Mirjalili, S. Mirjalili, S. Saremi, H. Faris, and I. Aljarah, "Grasshopper optimization algorithm for multi-objective optimization problems," *Applied Intelligence*, vol. 48, pp. 805-820, 2018, https://doi.org/10.1007/s10489-017-1019-8.

[40] M. A. AL-Ali, O. F. Lutfy, and H. Al-Khazraji, "Comparative study of various controllers improved by swarm optimization for nonlinear active suspension systems with actuator saturation," *International Journal of Intelligent Engineering and Systems*, vol. 17, no. 4, pp. 870-881, 2024, https://doi.org/10.22266/ijies2024.0831.66.

[41] T. O. Hodson, "Root mean square error (RMSE) or mean absolute error (MAE): When to use them or not," *Geoscientific Model Development*, vol. 15, pp. 5481-5487, 2022, https://doi.org/10.5194/gmd-15-5481-2022.